Ultrafast dynamic holography in nanocrystal solids

B. Kraabel, A. Malko, J. Hollingsworth, and V. I. Klimov[a)]
Chemistry Division, C-6, MS-J585, Los Alamos National Laboratory, Los Alamos, New Mexico 87545

(Received 6 July 2000; accepted for publication 1 February 2001)

We report efficient dynamic gratings in close-packed solids of CdSe nanocrystals. These gratings are formed on the subpicosecond time scale and have diffraction efficiencies up to 0.5% for film thicknesses of ~0.5 μm. Nanocrystal solids combine the best features of inorganic semiconductors (large resonant nonlinearities and high photostability) and organic semiconducting polymers (chemical flexibility and tunability of optical properties by simple synthetic means). Additionally, nanocrystal solids allow precise control over the spectral position of the nonlinear optical response by simply varying the size of the nanocrystals used in fabricating the solid (quantum confinement effect). © *2001 American Institute of Physics.* [DOI: 10.1063/1.1358365]

Holographic dynamic gratings are principal elements in a variety of optical devices used in optical communication and optical information processing.[1–3] Several different classes of materials with different types of nonlinearities have been used to demonstrate dynamic gratings.[1] Most extensively studied are materials that exhibit the photorefractive (PR) effect, such as PR inorganic crystals[4] and PR semiconductor quantum wells.[5] Recently, significant attention has been paid to organic polymers.[2] An attractive feature of polymers is the ease of manipulating their optical properties by simple chemical means such as chemical substitution. Polymeric materials with different mechanisms for optical nonlinearities (PR effect, resonant carrier excitation, charge transfer, etc.) have been fabricated and studied.[2,3,6,7]

In this letter, we report the use of solid-state films of close-packed semiconductor nanocrystals (NCs) in ultrafast dynamic holography. Semiconductor NCs are nanoscale particles with sub-10 nm dimensions.[8] Due to quantum confinement, the energy gap in a NC is a strong function of its radius R, with a confinement term that scales approximately as $1/R^2$. This strong size dependence makes it possible to tune the optical response of NCs (e.g., emission and absorption wavelengths) by simply changing the NC size. NCs can be chemically manipulated like large molecules and can be incorporated into polymer and glass matrices and into different photonic structures, including optical fibers, microcavities, photonic crystals, etc.

NCs exhibit large band-edge optical nonlinearities that are primarily due to state filling and Coulomb multiparticle interactions (carrier-induced Stark effect).[9] Excitation of a single electron–hole ($e-h$) pair per NC leads to ~40% bleaching of the band-edge optical transition.[9] In contrast to organic molecules that easily degrade under intense illumination, NCs are characterized by excellent long-term photostability due to the strong chemical bonding characteristic of inorganic semiconductors. Large optical nonlinearities, size-controlled spectral tunability, chemical flexibility, and a high level of photostability make NC materials extremely attractive for applications in linear and nonlinear optical devices, including those utilizing ultrafast holographic gratings.

In this work, we used surface-capped CdSe NCs fabricated by solution-based organometallic synthesis as described in Ref. 10. To achieve high concentrations of semiconductor material in the sample, we prepared close-packed NC films (thickness from 0.3 to 2 μm) by drop casting followed by evaporation of the solvent. In this work, we studied samples made of NCs with mean radii 1.2 and 2.1 nm (size dispersion 5% and 7%, respectively). Assuming random close packing, and taking into account the 1.1 nm thickness of the organic capping layer, we estimate the volume fraction of the semiconductor in the samples as ~20% for NCs with $R=1.2$ nm and ~30% for NCs with $R=2.1$ nm.

The experimental setup used to study dynamic gratings in NC solids is similar to that used previously.[7] Briefly, two 400 nm, 100 fs pump pulses crossed at the angle of 22° interfere at the sample plane to form an intensity grating. This in turn forms a population grating in the NC sample, which modulates its absorption (i.e., the imaginary part of the refractive index) via such mechanisms as state filling (leading to photoinduced bleaching of optical transitions) and the carrier-induced Stark effect (leading to transition shifts and modifications in oscillator strength).[9] The real part of the refractive index is modified through causality (Kramers–Kronig transformation). Thus, in general, we form mixed gratings (both real and imaginary parts of the refractive index are modulated), although in certain spectral regions we find either almost pure absorption or almost pure phase gratings, as discussed below. The dynamic grating formed in the samples was probed at the Bragg angle[1] (θ_0) with tunable 100 fs pulses generated by an optical parametric amplifier. The diffraction efficiency η was calculated as the ratio of the intensities of the diffracted and incident beams. The results reported here were obtained at 77 K, as cooling of the sample allowed us to increase the threshold for film optical damage. Room-temperature data were essentially equivalent.

In Fig. 1 we compare the linear absorption spectrum (solid line) with the spectra of the diffraction efficiency of the sample with $R=2.1$ nm measured at 1 ps (circles) and 3

a)Author to whom correspondence should be addressed; electronic mail: klimov@lanl.gov

 © 2001 American Institute of Physics
Downloaded 29 Mar 2001 to 128.165.88.103. Redistribution subject to AIP copyright, see http://ojps.aip.org/aplo/aplcr.jsp

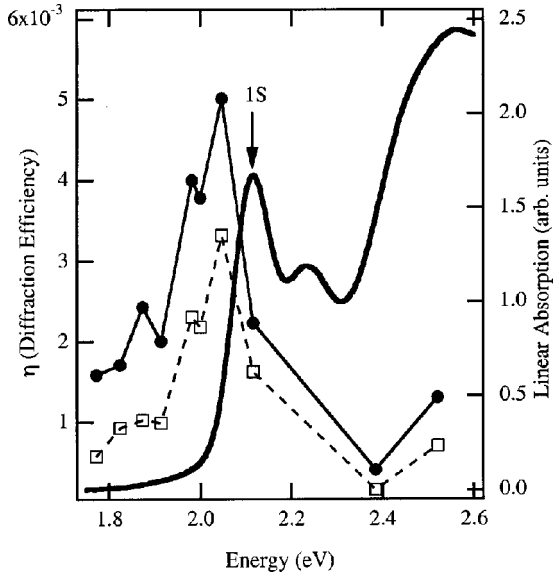

FIG. 1. Solid circles and open squares represent the diffraction efficiency at pump–probe delay times of 1 and 3 ps, respectively (left-hand axis). Thick solid line represents the linear absorption coefficient of the sample (right-hand axis).

ps (squares) after creating the grating (sample thickness was 0.4 μm). These data were taken at a pump fluence (coherent sum of the two pump beams) $J=10^{16}\,\mathrm{cm}^{-2}$, just below the threshold for optical damage of the sample. The peak diffraction efficiency of ~0.5% occurred at 2.05 eV, slightly below the band-edge absorption maximum (1*S* absorption)[9] located at 2.1 eV. The decay of the grating occurred on a sub-10 ps time scale (compare the 1 and 3 ps spectra in Fig. 1) and was spectrally nonuniform. The single-wavelength dynamics in Fig. 2 indicate that the decay is slower at the position of the 1*S* resonance (exponential constant of ~8 ps) and becomes faster on both sides of the 1*S* resonance (a more detailed analysis of the grating dynamics is given below).

Qualitatively, similar results were obtained for films made of NCs with $R=1.2$ nm. An important difference was that the positions of both the 1*S* absorption and the diffraction maximum were blueshifted by ~400 meV with respect to those for the 2.1 nm sample, which was due to a confinement-induced increase in the energy gap.

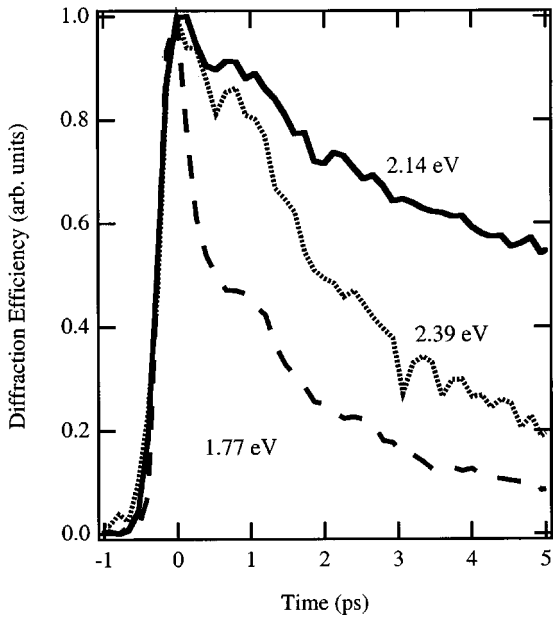

FIG. 2. Dynamics of the diffraction grating recorded at 2.39, 2.14, and 1.77 eV.

The combination of large diffraction efficiencies with ultrafast buildup/decay times of dynamic gratings is promising for applications in ultrafast dynamic holography. To compare the results obtained for NC solids with results previously reported for, e.g., polymeric materials, we use the temporal diffraction efficiency (TDE) as a figure of merit.[6,7] This quantity characterizes the material's performance in ultrafast holographic recording and is defined as η/τ_f, where τ_f is the formation time of the holographic grating. The maximum diffraction efficiency obtained in the present work (0.5%) combined with a grating formation time of 100 fs (Fig. 2), yields a TDE of $0.5\times10^{11}\,\mathrm{s}^{-1}$, which is comparable with the highest results reported for polymeric materials.[6,7] In addition to large TDE numbers, NC films offer the advantage of excellent photostability that is a serious concern, for example, for π-conjugated polymers.[11] In our experiments with NC samples, we did not observe any signs of photodegradation for several hours of illumination at excitation densities corresponding to diffraction efficiencies greater than 0.1%.

The pump photon energy used in this work corresponded to strong interband absorption suggesting that the dynamic gratings studied were dominated by resonant nonlinearities (i.e., nonlinearities associated with absorption/refraction changes due to photoexcited carriers). In order to quantitatively analyze the role of these nonlinearities in the formation of holographic responses, we compared the experimental spectra of diffraction efficiency with those calculated based on the spectra of carrier-induced absorption changes that were independently measured by us using a transient absorption (TA) experiment (see, e.g., Ref. 9). Such analysis was also useful for separating the contributions to the grating from the real and imaginary parts of the index of refraction. The calculations were performed using coupled wave theory.[12] For a mixed grating, this theory yields the following expression for diffraction efficiency:

$$\eta=\exp\left(-\frac{2\alpha_0 d}{\cos\theta_0}\right)\left[\sin^2\left(\frac{\pi\Delta n d}{\lambda\cos\theta_0}\right)+\sinh^2\left(\frac{\Delta\alpha d}{2\cos\theta_0}\right)\right], \quad (1)$$

where α_0 is the spatial average over the diffraction grating of the linear absorption coefficient, d is the sample thickness, λ is the probe wavelength, Δn is the modulation in the real part of the index of refraction, and $\Delta\alpha$ is the modulation of the absorption coefficient. In order to calculate the diffraction efficiency over a broad spectral range, first α_0 and $\Delta\alpha$ were measured experimentally, then Δn was derived from $\Delta\alpha$ via the Kramers–Kronig transformation.

In Fig. 3, we compare the results of this calculation using the TA spectrum measured at 1 ps to the 1 ps experimental spectrum of the diffraction efficiency. Both the overall magnitude and the general spectral shape of the calculated result agree well with the experiment, confirming that the observed gratings were dominated by absorption/refraction changes due to resonant carrier excitation. By considering each term in Eq. (1) individually, we can determine if a

Downloaded 29 Mar 2001 to 128.165.88.103. Redistribution subject to AIP copyright, see http://ojps.aip.org/aplo/aplcr.jsp

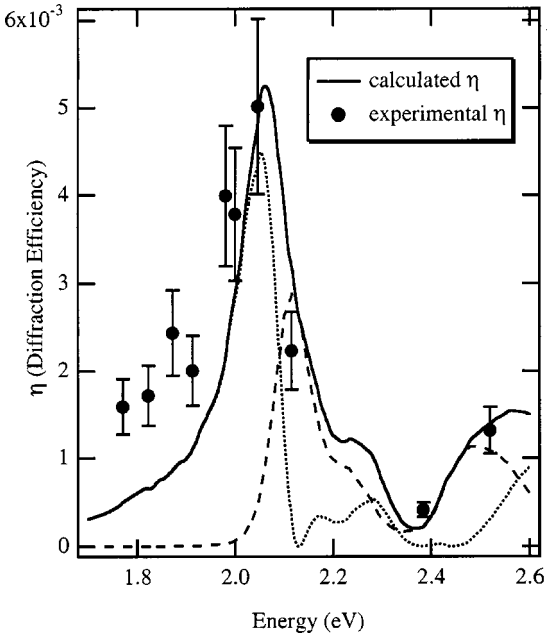

FIG. 3. Solid circles represent the experimentally measured diffraction efficiency at 1 ps. Thin solid line is the spectrum of diffraction efficiency calculated using Eq. (1) and experimental spectra α_0 and $\Delta\alpha$ (measured at 1 ps after excitation). The dotted and dashed lines represent the decomposition of the total difraction efficiency into contributions due to the phase and absorption modulations, respectively.

given spectral region is dominated by a pure phase or pure absorption grating, or by a mixed grating. The dotted and dashed lines in Fig. 3 show the contributions of the pure phase and pure absorption gratings, respectively. The diffraction grating is almost a pure absorption grating in the range of the $1S$ absorption maximum (see Fig. 3), consistent with the fact that the dominant effect of photoexcitation in NCs is bleaching of the $1S$ resonance.[9] Above and below the $1S$ absorption, the grating becomes mixed, and at the lower energies (within the NC energy gap) is dominated by phase modulation.

The dynamics of diffracted signals observed in these experiments can be qualitatively understood based on previous results for the dynamics of band-edge nonlinear optical responses in NCs obtained in TA studies.[9] In particular, the ultrafast grating formation time ($\sim$100 fs) is due to the fact that both mechanisms dominating band-edge optical nonlinearities in NCs (the carrier-induced Stark effect and state filling) have very short buildup times. The Stark effect is due to internal fields associated with photoexcited carriers and develops on a time scale determined by the duration of the laser pulse. The buildup of state-filling signals is determined by intraband relaxation and occurs on the sub-500 fs time scale.[9]

The decay dynamics of the diffraction grating exhibit two components: an initial fast component and a delayed slower component observed as a ''bump'' at approximately 1 ps after creating a grating (Fig. 2). This behavior can be explained in terms of a superposition of population dynamics of the lowest ($1S$) and the first-excited ($1P$) electron states. Because of a high spectral density of valence-band states, photoinduced absorption changes in CdSe NCs are dominated by populations of electron quantized levels.[9] Estimating the average number of $e-h$ pairs generated per NC (N) from $N=J\sigma_0$ (σ_0 is the NC absorption cross section estimated according to Ref. 9), we find $N\approx 8$ for the pump fluence used in the present experiments. Under quasithermal equilibrium (at times $>$500 fs), this corresponds to the situation where both the $1S$ (twofold degenerate) and $1P$ (sixfold degenerate) states are fully occupied. The fast initial decay of the diffracted signals is likely due to a rapid depopulation of the $1P$ level via multiparticle Auger recombination.[13] Using size-dependent data for Auger times from Ref. 13, we can estimate the eight $e-h$ pair lifetime to be $\sim$2 ps, consistent with the initial fast ps decay of the transient grating. The delayed component in the diffracted signals is likely due to the $1S$ carriers. Its slower dynamics can be explained by the existence of a ''$1P$ reservoir'' of high-energy carriers that continually replenish the $1S$ level until the number of $e-h$ pairs per NC drops below 2. This interpretation is consistent with the fact that the delayed component is not observed at pump levels below two $e-h$ pairs per NC. Additionally, the delayed component is most pronounced near the $1S$ transition. It drops in amplitude on both sides of the $1S$ resonance, but is still easily discernable because of the contribution to the grating of the index modulation which is determined by an integral over all energy levels.

In conclusion, we have demonstrated the use of NC solids as the active material for generating dynamic holographic gratings. The gratings are formed on the sub-ps time scale and offer a high diffraction efficiency of $\sim$0.5% for films of $\sim$0.5 μm thickness. The spectral maximum of diffraction efficiency is located in the vicinity of the lowest $1S$ absorption maximum (the NC band edge) and is tunable over a wide range by varying the size of the NCs used in fabricating the solid.

This research was supported by Los Alamos Directed Research and Development funds, under the auspices of the U.S. Department of Energy, and by the Air Force Office of Scientific Research, under Contract No. MIPR-99-0026.

[1] H. Eichler, P. Gunter, and D. Pohl, *Laser-Induced Dynamic Gratings* (Springer, New York, 1986).
[2] W. E. Moerner, A. Grunnet-Jepsen, and C. L. Thompson, Annu. Rev. Mater. Sci. **27**, 585 (1997).
[3] C. Halvorson, A. Hays, B. Kraabel, R. Wu, R. Wudl, and A. J. Heeger, Science **265**, 1215 (1994).
[4] *Electro-Optic and Photorefractive Materials*, edited by P. Günter (Springer, New York, 1987).
[5] Q. N. Wang, R. M. Brubaker, D. D. Nolte, and M. R. Melloch, J. Opt. Soc. Am. B **9**, 1626 (1992).
[6] E. Maniloff, D. Vacar, D. McBranch, H.-L. Wang, B. Mattes, J. Gao, and A. Heeger, Opt. Commun. **141**, 243 (1997).
[7] B. Kraabel, D. McBranch, B. Hseih, and F. Wudl, Synth. Met. **101**, 281 (1998).
[8] A. P. Alivisatos, Science **271**, 933 (1996).
[9] V. I. Klimov, Chem. Phys. B **104**, 6112 (2000).
[10] C. Murray, D. Norris, and M. Bawendi, J. Am. Chem. Soc. **115**, 8706 (1993).
[11] V. I. Klimov, D. W. McBranch, N. Barashkov, and J. Ferraris, Phys. Rev. B **58**, 7654 (1998).
[12] H. Kogelnik, Bell Syst. Tech. J. **48**, 2909 (1969).
[13] V. I. Klimov, A. A. Mikhailovsky, D. W. McBranch, C. A. Leatherdale, and M. G. Bawendi, Science **287**, 1011 (2000).

Downloaded 29 Mar 2001 to 128.165.88.103. Redistribution subject to AIP copyright, see http://ojps.aip.org/aplo/aplcr.jsp